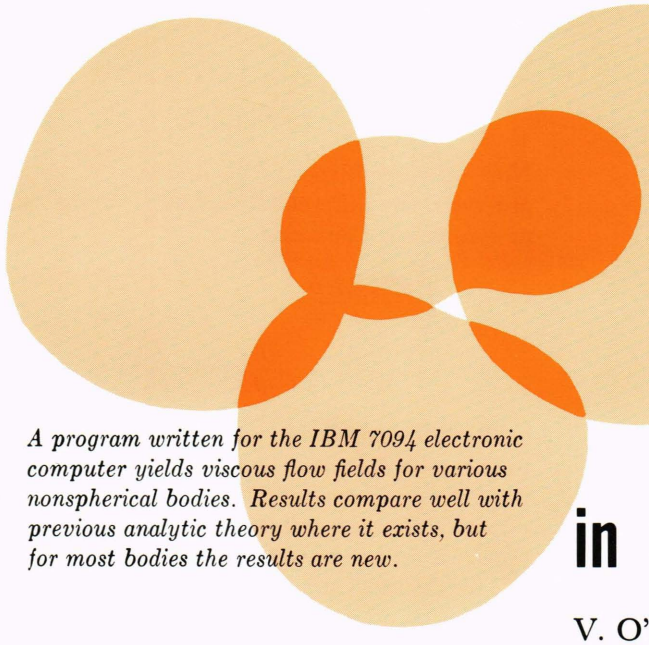

EGGS and other DEFORMED SPHEROIDS in STOKES FLOW

A program written for the IBM 7094 electronic computer yields viscous flow fields for various nonspherical bodies. Results compare well with previous analytic theory where it exists, but for most bodies the results are new.

V. O'Brien

Since antiquity the sphere has been regarded as the perfect shape—an object of classic beauty. It is entirely fitting that the classic theoretical solution of hydrodynamics is the viscous flow about a sphere given by G. G. Stokes in 1850.[1] Stokes' solution correctly predicted the drag force on a sphere for slow viscous flows. In honor of that feat all very slow flows have since been called Stokes flows. This note presents the numerical electronic computer program that has been developed to give the Stokes flow field for bodies of revolution of rather arbitrary cross-sectional shape.[2] The shape illustrations show some bodies that have been used in the program. They can be identified as shapes of eggs, apples, pears, dumbbells, etc., or by more mathematical definitions.

Of course, in the century since Stokes, Stokes flow solutions for nonspherical bodies have been sought by many others. Success has been attained for a few bodies: ellipsoid,[3] lens,[4] hemisphere,[4] and a hemispherical cap.[5] The general analytical problem of an arbitrary shape is quite difficult. Recently some steps toward generalization have been made by a linear perturbation technique.[6] This technique is limited to bodies that are only very slightly distorted spheroids. The bodies of revolution considered in our numerical program, by contrast, have deformations up to 50% or more of the undistorted radius. Bodies without rotational symmetry are excluded and the solution for a completely arbitrary shape is still a future goal. Many particle shapes of practical interest in several fields are covered by the present program.

Axisymmetry eases the mathematical task of solving the Stokes flow equation. (Note all the bodies in Refs. 4 and 5 are bodies of revolution.) The partial differential equation is closely related to the better known Laplacian equation that appears so often in physical problems. The Stokes equation and its solutions fall within the province of generalized axially symmetric potential theory.[7] In theory, any general Stokes solution can be used to meet the viscous nonslip boundary conditions

[1] G. G. Stokes, "On the Effect of the Internal Friction of Fluids on Pendulums," *Cambridge Philosophical Trans.*, **9**, 1850, 8–106. (Also in *Scientific Papers*, University Press, Cambridge, 1901.)

[2] V. O'Brien, "Stokes Flow About Deformed Spheroids," submitted for publication in *Chem. Eng. Sci.*

[3] A. Oberbeck, "Über Stationäre Flüssigkeit Bewegungen mit Berücksichtigung der Inneren Reibung," *Crelle Journal*, **81**, 1876, 62–80.

[4] L. E. Payne and W. H. Pell, "The Stokes Flow Problem for a Class of Axially Symmetric Bodies," *J. Fluid Mech.*, **7**, 1960, 529–549.

[5] W. D. Collins, "A Note on the Axisymmetric Stokes Flow of Viscous Fluid Past a Spherical Cap," *Mathematika*, **10**, 1963, 72–78.

[6] H. Brenner, "The Stokes Resistance of a Slightly Deformed Sphere," *Chem. Eng. Sci.*, **19**, 1964, 519–539.

[7] A. Weinstein, "On Tricomi's Equation and Generalized Axially Symmetric Potential Theory," *Bull. Acad. Roy. Belgique*, **37**, 1951, p. 348.

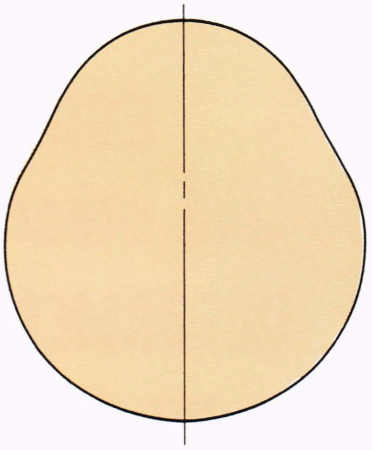

at the surface of any closed body. In practice, exact analytic solutions are hard to find and are likely to be very complex expressions.[4,5] Our computer program uses the general solution in spherical polar coordinates. The result, written as a finite series of simple terms, is only an approximation of the exact solution. However, uniqueness of the solution is guaranteed,[8] and the accuracy of the approximation can be checked.

For those interested in the details of the mathematics, the governing equation is

$$\frac{1}{\nu}\nabla\left(\frac{p}{\rho}+\phi\right)=\nabla^2\vec{u}\,. \qquad (1)$$

This is the steady momentum equation of incompressible fluid flow with the nonlinear inertial term neglected ($\vec{u}$ is the velocity vector, ϕ the potential of a conservative force field such as the gravity field, p the pressure, ρ the density, and ν the kinematic viscosity of the fluid). Axisymmetry allows the introduction of Stokes stream function ψ (proportional to the actual flux of fluid) in terms of the velocity components:

$$u_r=-\frac{1}{r^2\sin\theta}\frac{\partial\psi}{\partial\theta}\,,\quad v_\theta=\frac{1}{r\sin\theta}\frac{\partial\psi}{\partial r}\,,\quad w_\varphi\equiv 0\,. \qquad (2)$$

Here the spherical polar coordinate system (r, θ, φ) has been used. The vorticity vector $\vec{\omega}$ is the curl of $\vec{u}$, and in this axisymmetric case

$$\omega=\frac{1}{r\sin\theta}\left[\frac{\partial^2}{\partial r^2}+\frac{\sin\theta}{r^2}\frac{\partial}{\partial\theta}\left(\frac{1}{\sin\theta}\frac{\partial}{\partial\theta}\right)\right]\psi\,. \qquad (3)$$

Taking the curl of Eq. (1) and substituting Eq. (3), the "vorticity form" of the Stokes flow equation is obtained:

$$\left[\frac{\partial^2}{\partial r^2}+\frac{\sin\theta}{r^2}\frac{\partial}{\partial\theta}\left(\frac{1}{\sin\theta}\frac{\partial}{\partial\theta}\right)\right]^2\psi=0. \qquad (4)$$

Note the resemblance of the operator in this fourth order partial differential equation to that of the axisymmetric Laplacian,

$$\nabla^2\Phi=\left[\frac{\partial^2}{\partial r^2}+\frac{2}{r}\frac{\partial}{\partial r}+\frac{1}{r^2\sin\theta}\frac{\partial}{\partial\theta}\left(\sin\theta\frac{\partial}{\partial\theta}\right)\right]\Phi=0. \qquad (5)$$

The resemblance is not superficial or confined to the spherical polar coordinate system. Because the "Stokesian operator" and the Laplacian operator are intimately related, the similarity of form is apparent in all axisymmetric coordinate systems.[9]

The general spherical polar solution to Eq. (4) is

$$\psi=\sum_{n=2}^{\infty}\left(a_n r^{-n+1}+b_n r^{-n+3}+c_n r^n+d_n r^{n+2}\right)C_n^{-1/2}(\cos\theta)\,.$$

Here $C_n^{-1/2}(\cos\theta)$ is a Gegenbauer polynomial of order n and degree $(-1/2)$.[10] A uniform flow condition at infinity requires

$$\lim_{r\to\infty}\psi\to\frac{r^2}{2}(1-\cos^2\theta),$$

so all coefficients of higher positive powers of r are necessarily zero. The computer program uses

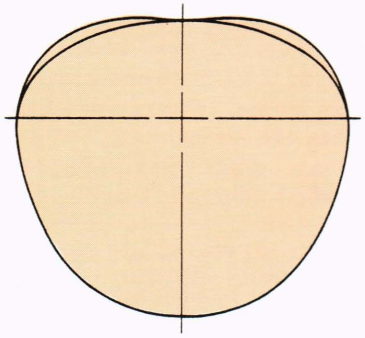

[8] R. Berker, "Integration des Equations du Mouvement d'un Fluide Visqueuse Incompressible," *Handbuch der Physik VIII/2*, Springer-Verlag, Berlin, 1963, p. 270.

[9] V. O'Brien, "Axi-Symmetric Magnetic Fields and Related Problems," *J. Franklin Inst.*, **275**, Jan. 1963, 24–35.

[10] W. Magnus and F. Oberhettinger, *Formulas and Theorems for the Functions of Mathematical Physics*, Chelsea Publishing Co., New York, 1954.

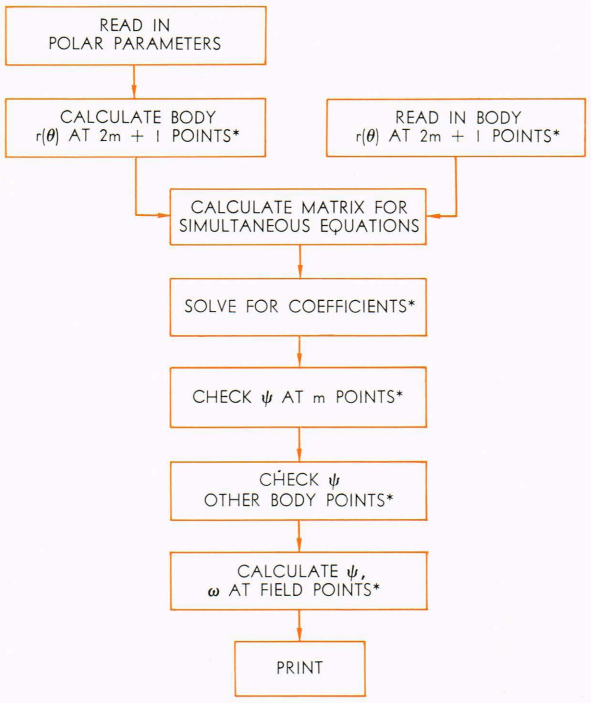

Fig. 1—Flow chart for numerical solution of Stokes flow field.

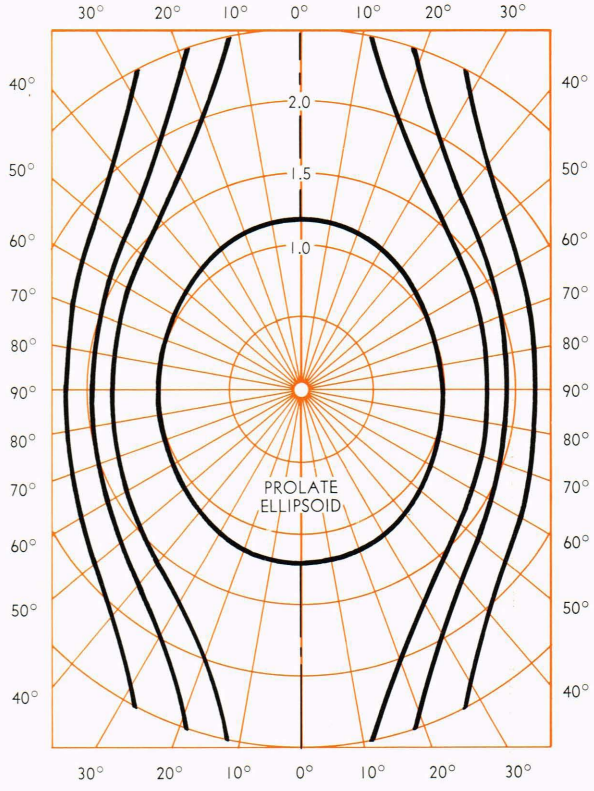

Fig. 2—Stream lines for a prolate ellipsoid of fineness ratio 1.2.

only a finite number of terms (m) or the approximate Stokes stream function solution

$$\psi = \frac{r^2}{2}(1-\cos^2\theta) + \sum_{n=2}^{m+1}(a_n r^{-n+1} + b_n r^{-n+3})\, C_n^{-1/2}(\cos\theta).$$

For a perfect sphere all except the coefficients a_2 and b_2 are zero.[1]

Program

In essence the numerical program satisfies the zero velocity condition at a number of points on

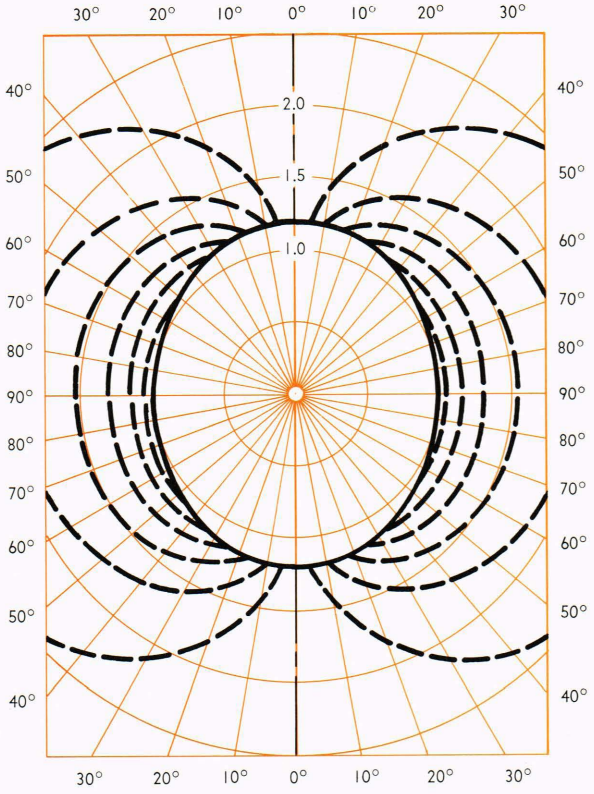

Fig. 3—Vorticity contours for a prolate ellipsoid of fineness ratio 1.2.

the body section. This determines a finite number of coefficients in the series expansion of the general solution. The approximate solution is first checked and then used to calculate stream lines and vorticity throughout the field. The details of the IBM 7094 FORTRAN program, as capably worked out by Mrs. Mary Lynam (APL), follow the flow chart in Fig. 1. The program is very short and fast; ten body cases are processed in 0.01 hr of machine time.*

* The smallest time unit that registers on the electronic computer.

The program first computes the radius as a function of angle θ from the given polar equation of the body section at $2m + 1$ values of θ, or it accepts the points $r(\theta)$ read in from a polar plot of the body. A typical value of $m = 10$ gives accurate results for many bodies, and the numbers below apply to this m. The boundary conditions (both velocity components equal zero) are expressed in terms of the series solution for the stream function ψ :

$$\frac{\partial\psi}{\partial(\cos\theta)} = 0 = -r^2\cos\theta - \sum_{n=2}^{m+1} (a_n r^{-n+1} + b_n r^{-n+3}) P_{n-1}(\cos\theta),$$

and

$$\frac{\partial\psi}{\partial r} = 0 = r\,(1-\cos^2\theta) + \sum_{n=2}^{m+1} [(-n+1)\,a_n r^{-n} + (-n+3)\,b_n r^{-n+2}]\, C_n^{-1/2}(\cos\theta).$$

(For computational purposes the Legendre polynomials and the Gegenbauer polynomials can be expressed in terms of hypergeometric functions.) This leads to twenty simultaneous equations to set twenty coefficients (written as a 20×21 matrix). The equations are solved for the coefficients by a double precision iterative scheme. The solution containing these coefficients is used to check the value of the stream function ψ back at the points used in the matrix calculation. (This checks the accuracy of the matrix and the inversion process.) The stream function ψ is also checked at ten intermediate body points not used in the matrix calculation. (This gives the accuracy of the approximate solution.) Finally, values of ψ and vorticity ω are calculated at specified points in the

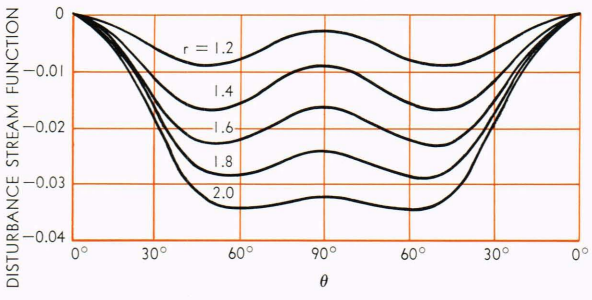

Fig. 4—Disturbance stream function for a prolate ellipsoid of fineness ratio 1.2.

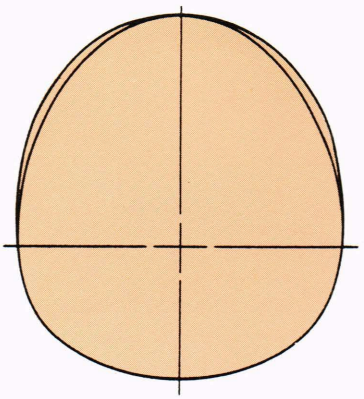

field (100 − 200 points). Printout usually consists of the starred boxes in Fig. 1, but other choices can be made.

Results

Many body shapes have been used in the program via the polar parameter input and the read-in option. As shown in Figs. 2, 3, and 4, the results can be displayed in many ways such as stream line plots, vorticity contours, or disturbance stream functions. (The last is the difference from the perfect-sphere solution.) Perhaps the simplest way to summarize the results is to plot the viscous drag value as it varies with the deformation of the spheroid. Also the drag is the quantity most easily obtained from experiments.

Figure 5 shows the calculated drag values for a series of prolate and oblate bodies. The bodies are slightly larger than the inscribed prolate and oblate ellipsoids even though they have the same axial dimensions. As expected from a theorem of

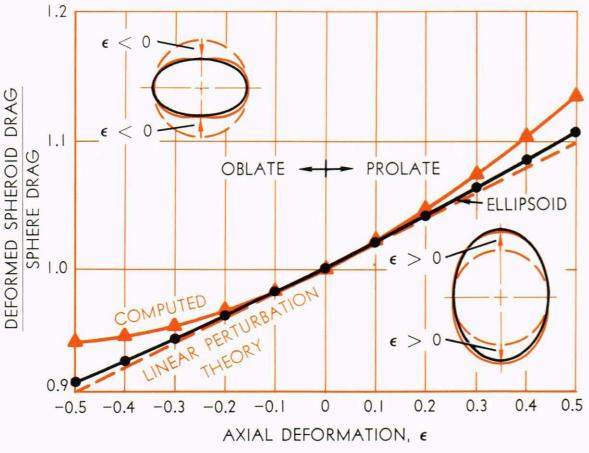

Fig. 5—Calculated drag values for a series of prolate and oblate bodies.

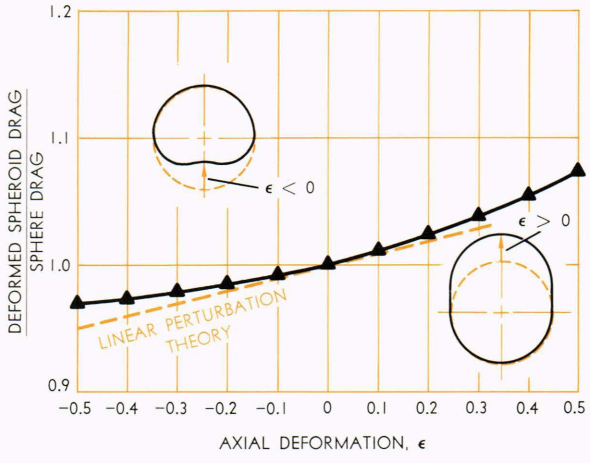

Fig. 6—Calculated drag values for bodies having one hemisphere deformed prolately or oblately.

Hill and Power,[11] the drag values are larger than the ellipsoid drag values. Both the exact analytic drag values and the ones determined numerically are shown for the ellipsoids. For very small deformations the linear perturbation theory (Ref. 6) is valid, but not for the larger deformations. For deformations small enough for the linear theory to hold, the prolate (or oblate) body is indistinguishable from the prolate (or oblate) ellipsoid.

Figure 6 shows the calculated drag values for bodies that have just one hemisphere deformed prolately or oblately. The linear perturbation theory predicts in this case one half of the drag increase (or decrease) of the prolate (or oblate)

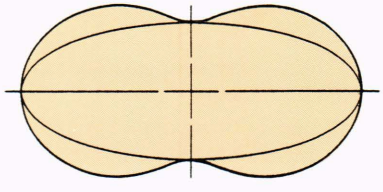

bodies above. The drag change is not linear with the amount of deformation beyond small values. Nevertheless, the drag change of the half-deformed object remains very close to one-half that of the evenly deformed one.

The drag ratios shown in Figs. 5 and 6 are normalized to the drag of the undeformed sphere. Since the equator of the sphere has not been changed in the deformations, the same ratio holds for the drag coefficients. (The drag coefficient is the drag divided by one-half the product of

[11] R. Hill and G. Power, "Extremum Principles for Slow Viscous Flow and the Approximate Calculation of Drag," *Quart. J. Mech. and Appl. Math.*, **9**, 1956, 313–319.

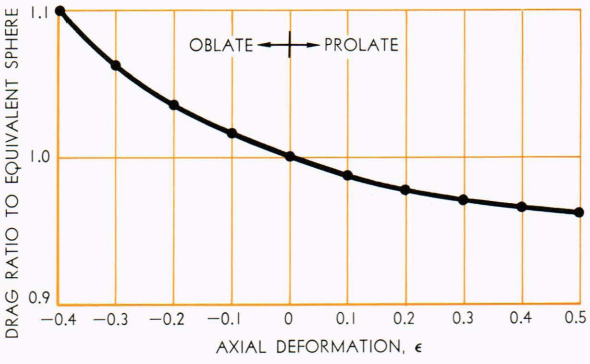

Fig. 7—Comparison of computed ellipsoid drag to drag of equivalent spheres.

frontal area, density, and velocity squared.) However, the drag for nonspherical particles is often expressed in relation to the drag of the sphere with equal volume, the so-called equivalent sphere. Prolate bodies with the same equatorial area have more volume than the unit sphere, and conversely, oblate bodies have less. The volume of the equivalent sphere rises more rapidly with the deformation parameter ϵ than the normalized drag value. Therefore, the prolate bodies have less drag than the equivalent spheres, and the oblate bodies more (Fig. 7).

Plots similar to Figs. 5 and 6 have been prepared for other classes of deformed spheroids. The curve of the calculated values of the drag coincides with the linear prediction for very small deformations. The relative drag values of bodies of different classes are in accord with the Hill-Power theorem.

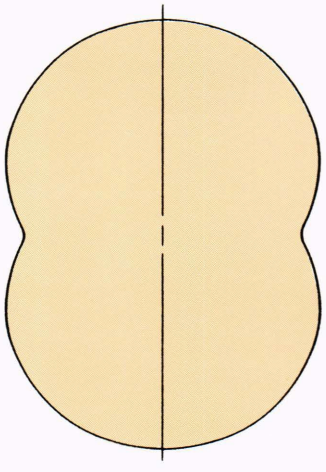

For very large deformations the values of the coefficients computed for the ten terms of the approximate flow solution do not diminish very rapidly with n. This shows that the exact (infinite series) expansion converges very slowly and

that not enough terms have been retained for an accurate approximation. The stream function checks confirm the inaccuracy of the approximation in these cases. Likewise, body shapes with convoluted or corrugated edges do not yield valid solutions with so few terms. However, it is possible in many cases to provide reliable lower and upper bounds on the drag value that differ by just several percent from $m = 10$ calculations (Figs. 8 and 9). The value of m can be increased to provide more accurate numerical solutions.†

Quite similar calculations can also be undertaken with the general series solution written in spheroidal coordinates (Ref. 4). The form of the solution is more complicated, but each term can be programmed for the electronic computer. The matrix operations would then be exactly as for the spherical solution. The convergence of the finite spheroidal approximation would be much more rapid for bodies that resemble spheroids with high eccentricity. Thus, a program written in spheroidal coordinates would permit Stokes flow solutions for spheroids more grossly deformed than the ones discussed here.

† However, increasing m without limit will probably reach a point of diminishing return due to inherent roundoff errors.

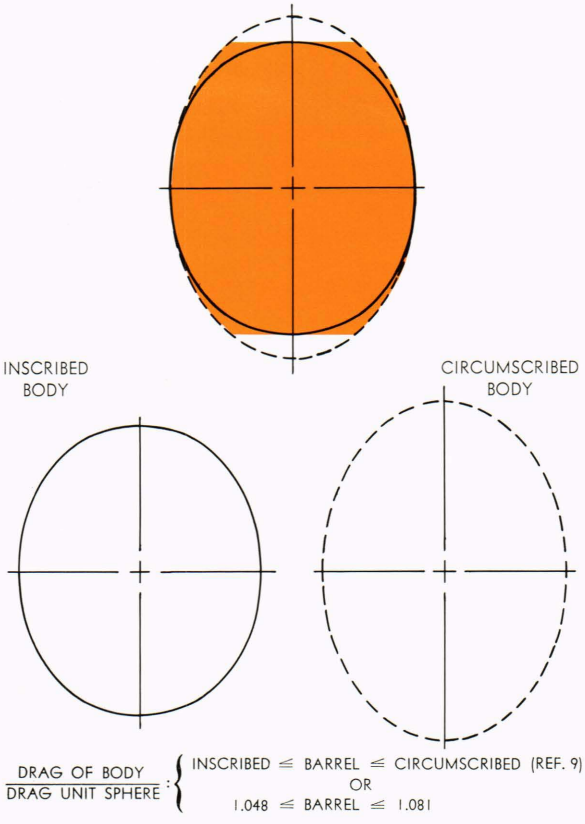

Fig. 8—Drag estimate for a barrel.

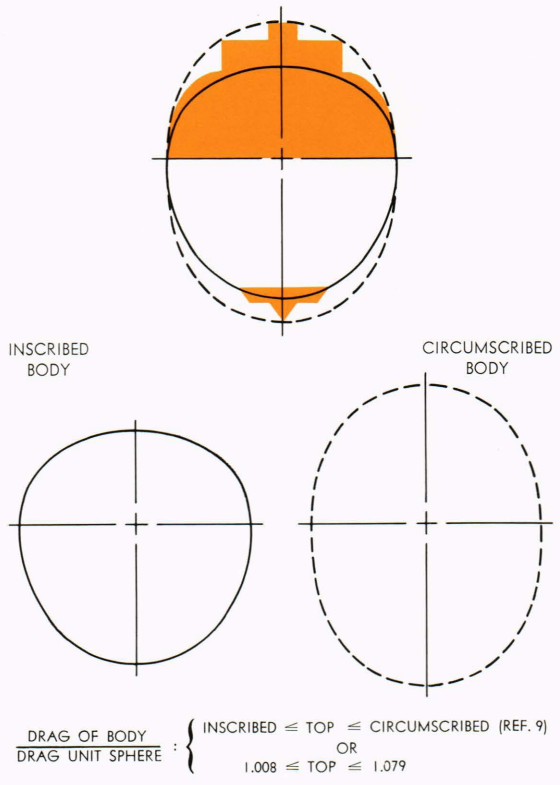

Fig. 9—Drag estimate for a top.

Conclusion

The speed and capacity of the modern electronic computer allow the solution of Stokes flow problems for a wide array of body shapes. The straightforward program gives accurate velocity fields for bodies that are impractical to handle by direct analytical methods. It gives drag values to high accuracy for these body shapes, and drag estimates for a larger class of bodies.

The flow range is limited to very low Reynolds number flows by the neglect of the inertial term in the flow equation. This limitation, somewhat a handicap to engineering use, can be overcome by further calculations using the full momentum equation. The detailed computations have not yet been carried out for all these bodies. However, on the basis of Refs. 12 and 13, the increased drag due to the inertial effect is simply a multiple of the Stokes drag calculated by this numerical program for bodies with fore-and-aft symmetry. For bodies without this symmetry, the inertial drag effect requires further calculation.

[12] V. O'Brien, *Axisymmetric Viscous Flows Correct to the First Order in Reynolds Number*, CM-1003, The Johns Hopkins University, Applied Physics Laboratory, Oct. 1961.

[13] W. Chester, "On Oseen's Approximation," *J. Fluid Mech.*, **13**, 1962, 557–569.